Biomedical Optics EXPRESS

An analytical method for predicting the geometrical and optical properties of the human lens under accommodation

Conor J. Sheil,[1,*] **Mehdi Bahrami**[2] **and Alexander V. Goncharov**[1]

[1]*Applied Optics Group, School of Physics, National University of Ireland, Galway, University Road, Galway, Ireland*
[2]*Faculty of Science, Engineering and Computing, Kingston University London, Penrhyn Road, Kingston upon Thames, KT1 2EE, UK*

[*]*c.sheil1@nuigalway.ie*

Abstract: We present an analytical method to describe the accommodative changes in the human crystalline lens. The method is based on the geometry-invariant lens model, in which the gradient-index (GRIN) iso-indicial contours are coupled to the external shape. This feature ensures that any given number of iso-indicial contours does not change with accommodation, which preserves the optical integrity of the GRIN structure. The coupling also enables us to define the GRIN structure if the radii and asphericities of the external lens surfaces are known. As an example, the accommodative changes in lenticular radii and central thickness were taken from the literature, while the asphericities of the external surfaces were derived analytically by adhering to the basic physical conditions of constant lens volume and its axial position. The resulting changes in lens geometry are consistent with experimental data, and the optical properties are in line with expected values for optical power and spherical aberration. The aim of the paper is to provide an anatomically and optically accurate lens model that is valid for 3 mm pupils and can be used as a new tool for better understanding of accommodation.

OCIS codes: (080.1010) Aberrations (global), (080.2468) First-order optics, (330.4460) Ophthalmic optics and devices, (330.5370) Physiological optics, (330.7322) Visual optics, accommodation, (330.7326) Visual optics, modelling.

References and links

1. H. von Helmholtz, *Handbuch der Physiologischen Optik* (Leopold Voss, 1867).
2. Y. Shao, A. Tao, H. Jiang, M. Shen, J. Zhong, F. Lu, and J. Wang, "Simultaneous real-time imaging of the ocular anterior segment including the ciliary muscle during accommodation," Biomedical Optics Express **4**, 466–480 (2013).
3. K. Richdale, L. T. Sinnott, M. A. Bullimore, P. A. Wassenaar, P. Schmalbrock, C.-Y. Kao, S. Patz, D. O. Mutti, A. Glasser, and K. Zadnik, "Quantification of age-related and per diopter accommodative changes of the lens and ciliary muscle in the emmetropic human eye," Investigative Ophthalmology & Visual Science **54**, 1095–1105 (2013).
4. A. de Castro, S. Ortiz, E. Gambra, D. Siedlecki, and S. Marcos, "Three-dimensional reconstruction of the crystalline lens gradient index distribution from OCT imaging," Optics Express **18**, 21905–21917 (2010).
5. A. de Castro, J. Birkenfeld, B. Maceo, F. Manns, E. Arrieta, J.-M. Parel, and S. Marcos, "Influence of shape and gradient refractive index in the accommodative changes of spherical aberration in nonhuman primate crystalline lenses," Investigative Ophthalmology & Visual Science **54**, 6197–6207 (2013).

#202310 - $15.00 USD Received 3 Dec 2013; revised 19 Feb 2014; accepted 18 Mar 2014; published 28 Apr 2014

6. A. Gullstrand, *Appendix IV of Treatise on Physiological Optics*, vol. 1 (Dover Phoenix Editions, 2005).
7. Y. Le Grand and S. G. El Hage, *Physiological Optics* (Springer–Verlag, 1980).
8. J. W. Blaker, "Toward an adaptive model of the human eye," Journal of the Optical Society of America **70**, 220–223 (1980).
9. R. Navarro, J. Santamaría, and J. Bescós, "Accommodation-dependent model of the human eye with aspherics," Journal of the Optical Society of America A **2**, 1273–1280 (1985).
10. G. Smith, P. Bedggood, R. Ashman, M. Daaboul, and A. Metha, "Exploring ocular aberrations with a schematic human eye model," Optometry & Vision Science **85**, 330–340 (2008).
11. H.-L. Liou and N. A. Brennan, "Anatomically accurate, finite model eye for optical modeling," Journal of the Optical Society of America A **14**, 1684–1695 (1997).
12. G. Smith, D. A. Atchison, and B. K. Pierscionek, "Modeling the power of the aging human eye," Journal of the Optical Society of America A **9**, 2111–2117 (1992).
13. M. Bahrami and A. V. Goncharov, "Geometry-invariant gradient refractive index lens: analytical ray tracing," Journal of Biomedical Optics **17**, 055001–1 – 055001–9 (2012).
14. A. V. Goncharov and C. Dainty, "Wide-field schematic eye models with gradient-index lens," Journal of the Optical Society of America A **24**, 2157–2174 (2007).
15. R. Navarro, F. Palos, and L. González, "Adaptive model of the gradient index of the human lens. i. formulation and model of aging ex vivo lenses," Journal of the Optical Society of America A **24**, 2175–2185 (2007).
16. G. Smith, "The optical properties of the crystalline lens and their significance." Clinical & Experimental Optometry **86**, 3–18 (2003).
17. C. Jones, D. Atchison, R. Meder, and J. Pope, "Refractive index distribution and optical properties of the isolated human lens measured using magnetic resonance imaging (MRI)," Vision Research **45**, 2352–2366 (2005).
18. E. A. Hermans, P. J. W. Pouwels, M. Dubbelman, J. P. A. Kuijer, R. G. L. van der Heijde, and R. M. Heethaar, "Constant volume of the human lens and decrease in surface area of the capsular bag during accommodation: An MRI and scheimpflug study," Investigative Ophthalmology & Visual Science **50**, 281–289 (2009).
19. C. E. Jones, D. A. Atchison, and J. M. Pope, "Changes in lens dimensions and refractive index with age and accommodation," Optometry & Vision Science **84**, 990–995 (2007).
20. R. Gerometta, A. C. Zamudio, D. P. Escobar, and O. A. Candia, "Volume change of the ocular lens during accommodation," American Journal of Physiology - Cell Physiology **293**, C797–C804 (2007).
21. S. A. Strenk, L. M. Strenk, J. L. Semmlow, and J. K. DeMarco, "Magnetic resonance imaging study of the effects of age and accommodation on the human lens cross-sectional area," Investigative Ophthalmology & Visual Science **45**, 539–545 (2004).
22. S. J. Judge and H. J. Burd, "The MRI data of strenk et al. do not suggest lens compression in the unaccommodated state (e-letter)," Investigative Ophthalmology & Visual Science **45**, 539 (2004).
23. R. A. Schachar, "The change in intralenticular pressure during human accommodation (e-letter)," Investigative Ophthalmology & Visual Science **45**, 539 (2004).
24. M. Dubbelman, G. V. der Heijde, and H. Weeber, "Change in shape of the aging human crystalline lens with accommodation," Vision Research **45**, 117–132 (2005).
25. S. Ortiz, P. Pérez-Merino, E. Gambra, A. de Castro, and S. Marcos, "In vivo human crystalline lens topography," Biomedical Optics Express **3**, 2471–2488 (2012).
26. R. Navarro, F. Palos, and L. M. González, "Adaptive model of the gradient index of the human lens. ii. optics of the accommodating aging lens," Journal of the Optical Society of America A **24**, 2911–2920 (2007).
27. C. E. Campbell, "Nested shell optical model of the lens of the human eye," Journal of the Optical Society of America A **27**, 2432–2441 (2010).
28. E. Lanchares, R. Navarro, and B. Calvo, "Hyperelastic modelling of the crystalline lens: Accommodation and presbyopia," Journal of Optometry **5**, 110–120 (2012).
29. M. Dubbelman and G. van der Heijde, "The shape of the aging human lens: curvature, equivalent refractive index and the lens paradox," Vision Research **41**, 1867–1877 (2001).
30. M. J. Howcroft and J. A. Parker, "Aspheric curvatures for the human lens," Vision Research **17**, 1217–1213 (1977).
31. D. Borja, D. Siedlecki, A. de Castro, S. Uhlhorn, S. Ortiz, E. Arrieta, J.-M. Parel, S. Marcos, and F. Manns, "Distortions of the posterior surface in optical coherence tomography images of the isolated crystalline lens: effect of the lens index gradient," Biomedical Optics Express **1**, 1331–1340 (2010).
32. F. Manns, V. Fernandez, S. Zipper, S. Sandadi, M. Hamaoui, A. Ho, and J.-M. Parel, "Radius of curvature and asphericity of the anterior and posterior surface of human cadaver crystalline lenses," Experimental Eye Research **78**, 39–51 (2004).
33. E. Hermans, M. Dubbelman, G. van der Heijde, and R. Heethaar, "Estimating the external force acting on the human eye lens during accommodation by finite element modelling," Vision Research **46**, 3642–3650 (2006).
34. R. Urs, F. Manns, A. Ho, D. Borja, A. Amelinckx, J. Smith, R. Jain, R. Augusteyn, and J.-M. Parel, "Shape of the isolated ex-vivo human crystalline lens," Vision Research **49**, 74–83 (2009).
35. J. F. Koretz, S. A. Strenk, L. M. Strenk, and J. L. Semmlow, "Scheimpflug and high-resolution magnetic resonance imaging of the anterior segment: a comparative study," Journal of the Optical Society of America A **21**,

#202310 - $15.00 USD Received 3 Dec 2013; revised 19 Feb 2014; accepted 18 Mar 2014; published 28 Apr 2014

346–354 (2004).
36. R. Urs, A. Ho, F. Manns, and J.-M. Parel, "Age-dependent fourier model of the shape of the isolated ex vivo human crystalline lens," Vision Research **50**, 1041–1047 (2010).
37. A. Ivanoff, "On the influence of accommodation on spherical aberration in the human eye, an attempt to interpret night myopia," Journal of the Optical Society of America **37**, 730–731 (1947).
38. M. Koomen, R. Tousey, and R. Scolnik, "The spherical aberration of the eye," Journal of the Optical Society of America **39**, 370–372 (1949).
39. T. Jenkins, "Aberrations of the eye and their effects on vision: 1. spherical aberration," The British journal of physiological optics **20**, 59 (1963).
40. D. A. Atchison, M. J. Collins, C. F. Wildsoet, J. Christensen, and M. D. Waterworth, "Measurement of monochromatic ocular aberrations of human eyes as a function of accommodation by the howland aberroscope technique," Vision Research **35**, 313–323 (1995).
41. M. J. Collins, C. F. Wildsoet, and D. A. Atchison, "Monochromatic aberrations and myopia," Vision Research **35**, 1157–1163 (1995).
42. J. He, S. Burns, and S. Marcos, "Monochromatic aberrations in the accommodated human eye," Vision Research **40**, 41–48 (2000).
43. S. Ninomiya, T. Fujikado, T. Kuroda, N. Maeda, Y. Tano, T. Oshika, Y. Hirohara, and T. Mihashi, "Changes of ocular aberration with accommodation," American Journal of Ophthalmology **134**, 924–926 (2002).
44. C. Hazel, M. Cox, and N. Strang, "Wavefront aberration and its relationship to the accommodative stimulus-response function in myopic subjects," Optometry & Vision Science **80**, 151–158 (2003).
45. H. Cheng, J. K. Barnett, A. S. Vilupuru, J. D. Marsack, S. Kasthurirangan, R. A. Applegate, and A. Roorda, "A population study on changes in wave aberrations with accomodation," Journal of Vision **4**, 272–280 (2004).
46. S. Plainis, H. S. Ginis, and A. Pallikaris, "The effect of ocular aberrations on steady-state errors of accommodative response," Journal of Vision **5**, 466–477 (2005).
47. Y. Wang, Z.-Q. Wang, H.-Q. Guo, Y. Wang, and T. Zuo, "Wavefront aberrations in the accommodated human eye based on individual eye model," Optik - International Journal for Light and Electron Optics **118**, 271–277 (2007).
48. E. Gambra, L. Sawides, C. Dorronsoro, and S. Marcos, "Accommodative lag and fluctuations when optical aberrations are manipulated," Journal of Vision **9**, 1–15 (2009).
49. Y.-J. Li, J. A. Choi, H. Kim, S.-Y. Yu, and C.-K. Joo, "Changes in ocular wavefront aberrations and retinal image quality with objective accommodation," Journal of Cataract & Refractive Surgery **37**, 835–841 (2011).
50. T. Young, "On the mechanism of the eye," Philosophical Transactions of the Royal Society of London **91**, 23–88 (1801).
51. N. López-Gil, V. Fernández-Sánchez, R. Legras, R. Montés-Micó, F. Lara, and J. L. Nguyen-Khoa, "Accommodation-related changes in monochromatic aberrations of the human eye as a function of age," Investigative Ophthalmology & Visual Science **49**, 1736–1743 (2008).
52. S. Kasthurirangan, E. L. Markwell, D. A. Atchison, and J. M. Pope, "In vivo study of changes in refractive index distribution in the human crystalline lens with age and accommodation," Investigative Ophthalmology & Visual Science **49**, 2531–2540 (2008).
53. G. Smith, D. A. Atchison, D. R. Iskander, C. E. Jones, and J. M. Pope, "Mathematical models for describing the shape of the in vitro unstretched human crystalline lens," Vision Research **49**, 2442–2452 (2009).
54. H. T. Kasprzak, "New approximation for the whole profile of the human crystalline lens," Ophthalmic & Physiological Optics **20**, 31–43 (2000).
55. S. Giovanzana, R. A. Schachar, S. Talu, R. D. Kirby, E. Yan, and B. K. Pierscionek, "Evaluation of equations for describing the human crystalline lens," Journal of Modern Optics **60**, 406–413 (2013).
56. S. G. El Hage and F. Berny, "Contribution of the crystalline lens to the spherical aberration of the eye," Journal of the Optical Society of America **63**, 205–211 (1973).
57. J. Sivak and R. Kreuzer, "Spherical aberration of the crystalline lens," Vision Research **23**, 59–70 (1983).
58. A. Tomlinson, R. P. Hemenger, and R. Garriott, "Method for estimating the spheric aberration of the human crystalline lens in vivo." Investigative Ophthalmology & Visual Science **34**, 621–629 (1993).
59. P. Artal and A. Guirao, "Contributions of the cornea and the lens to the aberrations of the human eye," Optics Letters **23**, 1713–1715 (1998).
60. T. Salmon and L. Thibos, "Relative contribution of the cornea and internal optics to the aberrations of the eye," Optometry & Vision Science **75**, 235 (1998).
61. P. Artal, A. Guirao, E. Berrio, and D. R. Williams, "Compensation of corneal aberrations by the internal optics in the human eye," Journal of Vision **1**, 1–8 (2001).
62. G. Smith, M. J. Cox, R. Calver, and L. F. Garner, "The spherical aberration of the crystalline lens of the human eye," Vision Research **41**, 235–243 (2001).
63. S. Amano, Y. Amano, S. Yamagami, T. Miyai, K. Miyata, T. Samejima, and T. Oshika, "Age-related changes in corneal and ocular higher-order wavefront aberrations," American Journal of Ophthalmology **137**, 988–992 (2004).
64. J. E. Kelly, T. Mihashi, and H. C. Howland, "Compensation of corneal horizontal/vertical astigmatism, lateral

#202310 - $15.00 USD Received 3 Dec 2013; revised 19 Feb 2014; accepted 18 Mar 2014; published 28 Apr 2014

coma, and spherical aberration by internal optics of the eye," Journal of Vision **4**, 262–271 (2004).
65. J. L. Alió, P. Schimchak, H. P. Negri, and R. Montés-Micó, "Crystalline lens optical dysfunction through aging," Ophthalmology **112**, 2022–2029 (2005).
66. M. Millodot and J. Sivak, "Contribution of the cornea and lens to the spherical aberration of the eye," Vision Research **19**, 685–687 (1979).
67. P. Artal, E. Berrio, A. Guirao, and P. Piers, "Contribution of the cornea and internal surfaces to the change of ocular aberrations with age," Journal of the Optical Society of America A **19**, 137–143 (2002).
68. A. Glasser and M. C. Campbell, "Presbyopia and the optical changes in the human crystalline lens with age," Vision Research **38**, 209–229 (1998).
69. J. C. He, J. Gwiazda, F. Thorn, and R. Held, "Wave-front aberrations in the anterior corneal surface and the whole eye," Journal of the Optical Society of America A **20**, 1155–1163 (2003).
70. T. O. Salmon and L. N. Thibos, "Videokeratoscope-line-of-sight misalignment and its effect on measurements of corneal and internal ocular aberrations," Journal of the Optical Society of America A **19**, 657–669 (2002).
71. J. He, E. Ong, J. Gwiazda, R. Held, and F. Thorn, "Wave-front aberrations in the cornea and the whole eye," Investigative Ophthalmology & Visual Science **41**, S105 (2000).
72. H. Burd, S. Judge, and J. Cross, "Numerical modelling of the accommodating lens," Vision Research **42**, 2235–2251 (2002).

1. Introduction

The mechanism of accommodation in the human eye is still an area of on-going research. The most widely accepted theory is that proposed by Helmholtz in his *Handbuch der Physiologischen Optik* in 1867 [1]. This Helmholtzian theory of accommodation states that contraction of the ciliary muscle body reduces zonular and capsular tension, allowing the lens to form a steeper, more convex shape. This corresponds to the accommodated state, with an associated increase in lenticular refractive power; the accommodated state provides clear vision at near distances. For distant vision, the ciliary muscle relaxes (dilates), and as a result the lens is stretched into a thinner shape with reduced refractive power. This is the *un*accommodated state, in which the lens is kept under constant tension. Experimental support for this most commonly accepted Helmholtzian theory includes, amongst many others, an interesting paper by Shao *et al.* (2013) showing real-time imaging of accommodative changes in the anterior segment of the eye [2]. While experimental efforts show that lenticular spherical aberration (SA) becomes more negative with accomodation, it is clear that increasing surface curvatures cause more positive SA; thus the accommodative decrease in lenticular radii should produce more positive SA. We aim to investigate this apparent contradiction by looking at the lens' surface and gradient index contributions to lenticular SA.

The field of ocular biometry is fast improving, with new and enhanced imaging methods capable of taking more accurate data with better sampling. While wavefront sensing continues to provide high-quality measurement of ocular wavefront aberration, the improving temporal and spatial resolution of magnetic resonance imaging (MRI) [3] and optical coherence tomography (OCT) [4, 5] may help with obtaining additional biometric information. The availability of these more accurate instruments for ocular biometry allows one to develop more advanced optical and physical models of the human eye; in particular, the crystalline lens.

Historically, some of the first accommodative models of the human crystalline lens were provided by Gullstrand [6] and Le Grand [7], who gave parameters for the unaccommodated and fully-accommodated lens; however, they did not provide data for intermediate accommodative amplitudes. Their four-surface lens model lacks a GRIN structure and also does not employ aspheric surfaces. This model was extended to account for the intermediate states by Blaker in his 1980 paper [8], by assuming that the GRIN lens' radii, diameter and central thickness vary linearly with accommodation. In 1985, Navarro *et al.* [9] showed that the on-axis optical properties of the human eye can be reproduced using aspheric lenticular surfaces with an equivalent refractive index for the lens. The lens' geometrical parameters changed logarithmically with accommodation in their model, while a parabolic adjustment to the equivalent refractive

#202310 - $15.00 USD Received 3 Dec 2013; revised 19 Feb 2014; accepted 18 Mar 2014; published 28 Apr 2014

index was performed. More recently, Smith and co-workers [10] modelled the accommodating lens using a trial and error process, in which the lens' dimensions were altered linearly while keeping the volume constant; this led to a change in the lens' radii and asphericities. This model was based on the Liou–Brennan eye [11], which was presented only in the relaxed form; thus, the coefficients of the GRIN medium were also altered to account for accommodative effects. We can see, however, that these GRIN coefficients do not depend on surface asphericity.

It can be desirable to analyse accommodation-dependant optical properties of the human lens featuring gradient index in ray-tracing software such as Zemax. When starting with a set of data for the unaccommodated lens, currently one must predict what values the accommodated lens parameters will take. If, for example, the lenticular radii, conic constants and central thickness of the accommodated lens are inserted into the ray-tracing software, these accommodated parameters will not necessarily be optically or physically appropriate. That is, the accommodated lens will not display the correct power or SA, and it may have changed substantially in volume. The current study aims to develop an analytical method of describing the geometrical and optical changes in the lens under accommodation. In this paper, we describe an anatomically realistic, adjustable lens, which can be used as a tool for ocular modelling and understanding of accommodation.

2. Analytical method

An equation describing the variation of refractive index n within the human lens has been proposed by Smith *et al.* [12] as:

$$n(r) = c_0 + c_p r^p,$$

where r is the normalised radius in the equatorial section, c_0 is the refractive index at the center of the lens and c_p is the difference between the refractive indices at the center and surface of the lens. The parameter p extends the applicability of this GRIN representation as it may account for some optically significant age-related changes in the GRIN structure. This equation, for the case of the geometry-invariant lens model [13], can be rewritten as:

$$n(\zeta) = n_c + (n_s - n_c)(\zeta^2)^P,$$

where ζ is the normalized distance from the lens' centre, n_c and n_s are the refractive indices at the center and at the surface of the GRIN lens, respectively, and $P = p/2$.

The GRIN structure of this lens model is coupled to the shape of the external surface of the lens. This is an attractive feature for modelling the accommodative changes since it secures the optical integrity of the GRIN structure. The general outline of the GRIN medium can be visualised by looking at its iso-indicial contours, which are surfaces of constant refractive index; for example, Fig. 1 contains five iso-indicial contours with a refractive index step of 0.008. Preserving the optical integrity of the GRIN structure requires that the number of contours does not increase or decrease with accommodation. Few recent lens models [13–15] feature this coupling of GRIN structure and external lens shape. Of these recent models, we choose the geometry-invariant model [13] since it offers both a realistic GRIN distribution with the age-dependent parameter P and continuous iso-indicial surfaces. Note also that $n(\zeta)$ is a continuous function.

The external shape of the lens in this model is a conicoid of revolution with a higher-order aspheric term. The general form for a conicoid of revolution, written as a function of surface sag (z), is given by

$$\rho^2 = 2Rz - (1+K)z^2,$$

where R is the vertex radius of curvature, K is the conic constant and ρ is the perpendicular distance (height) from the optical axis z. The addition of an aspheric cubic term transforms the

#202310 - $15.00 USD Received 3 Dec 2013; revised 19 Feb 2014; accepted 18 Mar 2014; published 28 Apr 2014

surface profile into a *figuring conicoid function* [16]:

$$\rho^2 = 2Rz - (1+K)z^2 + Bz^3. \tag{1}$$

The first continuity condition states that $\rho_a(Z_c) = \rho_p(Z_c)$; where ρ_a and ρ_p are the respective heights of the anterior and posterior surface contours, and Z_c is the axial position of the lens equator. If we note that the *shape factor* of the lens' surfaces is given by $Q = 1+K$, we have the following:

$$\begin{aligned} &2R_a(T_a+Z_c) - Q_a(T_a+Z_c)^2 + B_a(T_a+Z_c)^3 = \\ &2R_p(T_p-Z_c) - Q_p(T_p-Z_c)^2 + B_p(T_p-Z_c)^3. \end{aligned} \tag{2}$$

where the subscripts a and p denote the anterior and posterior segments, respectively. As outlined in previous work by Bahrami and Goncharov [13], the constant B is chosen so that the second continuity condition $\frac{d\rho(z)}{dz}|_{Z_c} = 0$ is satisfied; i.e. the first derivative $d\rho/dz$ at the equatorial interface connecting the anterior and posterior surfaces is equal to zero, given by:

$$\begin{aligned} B_a &= \frac{2}{3}\frac{Q_a(T_a+Z_c) - R_a}{(T_a+Z_c)^2} \quad \text{and} \\ B_p &= \frac{2}{3}\frac{Q_p(T_p-Z_c) - R_p}{(T_p-Z_c)^2}. \end{aligned} \tag{3}$$

The position of the lens' equator (Z_c) relative to the centre of the nucleus can thus be calculated by inserting Eq. 3 into Eq. 2 to give the following:

$$\begin{aligned} Z_c = \frac{1}{Q_p - Q_a}\Big[&T_aQ_a + T_pQ_p - 2(R_a+R_p) + \\ &\sqrt{T^2Q_aQ_p - 4T(R_aQ_p + R_pQ_a) + 4(R_a+R_p)^2}\Big], \end{aligned} \tag{4}$$

where $T = T_a + T_p$ is the axial thickness of the lens. T_a and T_p are respectively defined as the anterior and posterior axial lens thicknesses relative to the centre of the lens nucleus.

Since T_a and T_p are positive quantities, and Z_c is a negative quantity [13], the anterior and posterior axial thicknesses (sags) of the lens are given by $Z_a = T_a + Z_c$ and $Z_p = T_p - Z_c$. The anterior and posterior sags are defined from their respective poles (vertices) to the lens *equator*, while distances T_a and T_p are defined from their respective poles to the centre of the nucleus. The centre of the nucleus is the position of peak refractive index and is defined as the origin; it is not necessarily at the same axial position as the lens' equator [15, 17]. See Fig. 1 for a visualisation of the two definitions.

Next, an analytical formula for the lens' volume can be derived using the disc method of integral calculus for the volume of a solid of revolution:

$$V = \pi\int_{-T_a}^{Z_c} \rho_a^2(z)\,dz + \pi\int_{Z_c}^{T_p} \rho_p^2(z)\,dz, \tag{5}$$

taking note again that T_a and T_p are positive, while Z_c is negative. Since the lenticular epithelial stroma constitutes a soft condensed medium and is essentially incompressible, it seemed reasonable to assume that the volume does not change on accommodation. A recent study by Hermans *et al*. came to the same conclusion experimentally [18]. Furthermore, the relatively short timescale over which the accommodation process occurs is rather short to facilitate any volume change through passage of water/aqueous into or out of the lens material [19]. A study by Gerometta *et al.* [20] found that bovine lenticular volume increases by 8% with accommodation, and expected the human lenticular volume to increase by 3%; however, one cannot be

#202310 - $15.00 USD Received 3 Dec 2013; revised 19 Feb 2014; accepted 18 Mar 2014; published 28 Apr 2014

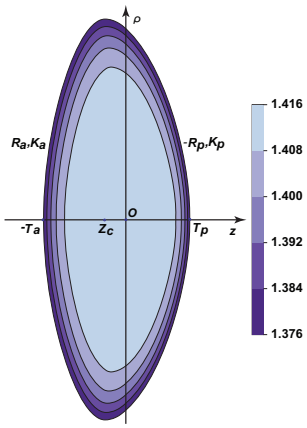

Fig. 1: Visualisation of T_a, T_p and Z_c in a GRIN lens; age-related parameter $P = 2.94$.

certain of the applicability of the bovine study to the human lens. Another study by Strenk *et al.* [21] concluded that the lenticular volume increases with accommodation, but there has been considerable discussion regarding the accuracy and validity of their method [22, 23]. In any instance, we anticipate a small change in lens volume which, although non-negligible, will not drastically affect the results of our model. Any future definitive answer for the accommodative change in lenticular volume can be incorporated into our analytical method.

In our present study, the constant volume condition is used as a control for the accommodated lens. The volume calculated using Eq. 5 is given below:

$$V = \frac{1}{6}\pi[5R_pZ_p^2 + 5R_aZ_a^2 - Q_pZ_p^3 - Q_aZ_a^3]. \tag{6}$$

3. Finding the conic constants of the lens

To demonstrate application of this analytical method, we use sample experimental data for the accommodative changes in lenticular radii and central thickness. We present an initial example using population-averaged Scheimpflug data from the work of Dubbelman *et al.* (2005) [24], which have consistently smaller error compared to data obtained with other imaging instruments, for example MRI [3, 18]. The application of these Scheimpflug data helps to ensure that the accommodative changes in radii and central thickness are anatomically realistic. The model is defined for a 30 year old lens, covering a range of accommodative amplitudes $A = 0$–8 D. In this example, the anterior and posterior radii of curvature and central lens thickness were calculated for each accommodative amplitude (in steps of 2 D, for clarity) using empirical linear equations given in Dubbelman *et al.* [24]. The change per dioptre in the anterior radius of curvature R_a, posterior radius of curvature R_p and central thickness T are:

$$\begin{aligned} R_a(A) &= R_{0a} + \Delta R_a = R_{0a} + (0.35 - 0.084R_{0a})A, \\ R_p(A) &= R_{0p} + \Delta R_p = R_{0p} + (0.37 - 0.082R_{0p})A, \\ T(A) &= T_0 + \Delta T = T_0 + (0.0436)A, \end{aligned} \tag{7}$$

where R_{0a}, R_{0p} and T_0 are the unaccommodated radii and thickness, and A is accommodative amplitude in D. Note that these equations represent the change in lenticular parameters per dioptre of stimulus. Objective accommodative response was not measured, and so these formulae may include accommodative lag.

#202310 - $15.00 USD Received 3 Dec 2013; revised 19 Feb 2014; accepted 18 Mar 2014; published 28 Apr 2014

Conic constants can only be accurately determined by imaging a relatively large diameter of the lens [16]. The accuracy in measuring the conic constants of the human lens' surfaces by Scheimpflug imaging is limited by lenticular occlusion by the finite maximum size of the iris and ocular refractive distortion. Consequently, the main motivation in our study was to find a way of predicting the conic constants of the human lens at different accommodative amplitudes, while the data for accommodative changes in the lenticular radii and central thickness were taken from the literature.

In order to develop an analytical method of finding the conic constants, we also use additional information for the accommodative changes in the anterior chamber depth (ACD) of the eye. As the lens accommodates, its anterior pole moves forward into the anterior chamber and this can be seen as a reduction in the ACD. In the same study by Dubbelman *et al.* [24], partial coherence interferometry was used to measure a change per dioptre in the anterior chamber of $\Delta ACD(A) = -0.036A$ mm for the 30 year old eye.

We use the relation above together with Eq. 7 as a basis for finding $R_a(A)$, $R_p(A)$ and $T(A)$, and $ACD(A)$ for a given accommodative amplitude. To find the anterior and posterior conic constants, we apply the following two conditions to the lens: constant volume (Eq. 6) and fixed equator position. The latter assumes that the equator of the lens does not move axially within the eye during accommodation; thus, the reduction in ACD can be seen as an increase in the anterior sag Z_a of the lens and can be expressed as:

$$Z_a(A) = Z_{0a} - \Delta ACD(A). \tag{8}$$

Finally, using Eqs. 4, 6 and 8, we can obtain the anterior and posterior conic constants as a function of accommodative amplitude:

$$K_a = \frac{\pi(T - Z_a)(R_p(T - Z_a) - R_a Z_a) - 6V_0}{\pi T Z_a^2} + \frac{5R_a}{Z_a} - 1, \quad \text{and} \tag{9}$$

$$K_p = \frac{\pi Z_a(R_a Z_a - R_p(T - Z_a)) - 6V_0}{\pi T(T - Z_a)^2} + \frac{5R_p}{T - Z_a} - 1. \tag{10}$$

Note that calculation of the initial volume V_0 requires sample data for R_{0a}, R_{0p}, K_{0a}, K_{0p} and T_0. Alternatively, if we have data for the accommodative change in K_a, we can solve Eq. 9 for Z_a, and subsequently find K_p from Eq. 10. This has physical significance since it allows us to predict, using data for K_a, the accommodative change in K_p, which is difficult to measure *in vivo*.

4. Analysis of lenticular geometry

We define the initial lens geometry based on the recent work of Ortiz *et al.* [25]. We used the following parameters for the unaccommodated lens: $R_{0a} = 12.48$ mm, $R_{0p} = 7.25$ mm, $T_0 = 3.18$ mm, $K_{0a} = -2.57$ and $K_{0p} = -1.64$. Assuming the centre of the lens' nucleus is located more posteriorly [15, 17, 26], we set $T_a = 0.6T$ and $T_p = 0.4T$, so that $T_{0a} = 1.91$ mm and $T_{0p} = 1.27$ mm.

These initial parameters allow us to calculate the geometrical features of the lens, which were derived analytically. First, the position of the lens' equator with respect to the centre of the nucleus is given by Eq. 4: $Z_{0c} = -0.74$ mm. Hence, we can calculate the anterior sag $Z_{0a} = T_{0a} + Z_{0c} = 1.17$ mm, the posterior sag $Z_{0p} = T_{0p} - Z_{0c} = 2.01$ mm and the two B coefficients: $B_{0a} = -6.93$ mm^{-1} and $B_{0p} = -1.41$ mm^{-1}. Finally, the initial volume V_0 is calculated using Eq. 6 to give $V_0 = 125.45$ mm^3. Using Eqs. 7, 3 and 8, we can calculate the parameters of the lens at different accommodative amplitudes, as shown in Tables 1 and 2 below for $A = 0$, 2, 4, 6 and 8 D. Figure 2 shows the transverse cross-section of the lens, with the anterior and posterior surfaces to the left and right, respectively—note that the lens is axisymmetric.

#202310 - $15.00 USD Received 3 Dec 2013; revised 19 Feb 2014; accepted 18 Mar 2014; published 28 Apr 2014

Table 1: Predicted changes in geometrical parameters of the lens under accommodation. All distances are in mm, with area in mm^2, and power is given in D.

A	R_a	R_p	T	Z_c	Z_a	Z_p	Eq. Diam.	Surf. Area	Refr. Power
0	12.48	7.25	3.18	−0.734	1.174	2.007	9.001	152.6	19.23
2	11.08	6.80	3.27	−0.715	1.246	2.021	8.911	150.6	20.93
4	9.687	6.35	3.35	−0.695	1.318	2.037	8.836	148.9	22.99
6	8.290	5.90	3.44	−0.675	1.390	2.052	8.774	147.6	25.58
8	6.893	5.45	3.53	−0.656	1.462	2.067	8.727	146.5	28.97

Table 2: Figuring and approximate conic constants of the lens' surfaces, and their contribution to SA. The change in SA per dioptre is calculated as a linear fit of the SA versus accommodation for the ranges 0–2 D, 0–4 D, 0–6 D and 0–8 D.

A (D)	B_a (mm^{-1})	B_p (mm^{-1})	K_a	K_p	K_a^*	K_p^*	ΔSA (μm/D) $W_{4,0}$	ΔSA (μm/D) Z_4^0	Linear fit range (D)
0	−6.93	−1.41	−2.57	−1.64	−0.83	−1.03			
2	−6.25	−1.48	−3.79	−2.12	−2.05	−1.45	−0.0470	−0.0035	0–2
4	−5.90	−1.56	−5.32	−2.64	−3.49	−1.90	−0.0684	−0.0051	0–4
6	−5.76	−1.65	−7.03	−3.21	−5.03	−2.38	−0.0993	−0.0074	0–6
8	−5.74	−1.76	−8.87	−3.81	−6.62	−2.89	−0.1516	−0.0113	0–8

The negative value of the conic constants, seen in Table 2, can be compared with the literature [24, 25, 27, 28]. The *in vivo* study of Dubbelman *et al.* [29] reports a value of -4.5 ± 2.8 for the anterior conic of the unaccommodated 30 year old lens, and a value of -2.9 ± 3.8 for the posterior conic. Ortiz *et al.* [25] show a range in averaged asphericities of 3 subjects; from -2.57 to -0.43 for the anterior conic, and -1.64 to -0.01 for the posterior conic. For the *in vitro* lens (assumed to be fully accommodated), Howcroft and Parker [30] show that both the anterior and posterior surfaces varied widely with hyperbolic, parabolic and elliptical profiles for 60 cadaver eyes. Judging by the figures presented in the work of Borja *et al* [31], the asphericity of the anterior surface ranges between -14 and $+2$; that of the posterior surface ranges between -2 and $+2$. The work of Manns *et al.* [32] produces an average of 3.27 ± 2.01 for the anterior conic, and -1.64 ± 1.85 for the posterior conic of cadaver lenses. The average *in vitro* data are difficult to interpret, since the accommodative state is not well-defined. In terms of theoretical modelling, the lens of Smith *et al.* [10] (based on Liou and Brennan's [11]) shows a decrease in anterior and posterior conic constants from -0.94 to -0.955 and 0.96 to 0.471, respectively, with 3 D accommodation. The nested shell optical model of Campbell [27] indicates that the anterior and posterior conic constants have a value of -5.00 for the 25 year old lens. The finite element model of Lanchares *et al.* [28] shows that the anterior and posterior conic constants have values of -4 and -3, respectively, in the unaccommodated eye. For their finite element model, Hermans *et al.* [33] use values of -4 and -8 for the conic constants of the anterior surface at 0 D and 8 D respectively, while using a value of -3 for the posterior conic at both accommodative amplitudes; these values are based on the work of Dubbelman

#202310 - $15.00 USD Received 3 Dec 2013; revised 19 Feb 2014; accepted 18 Mar 2014; published 28 Apr 2014

and co-workers [24, 29]. The majority of these studies have shown the conic constants to be negative, with Dubbelman *et al.* [24] reporting that the conics become more negative with accommodation; our lens example shows a similar trend.

The volume of the lens can be compared with the experimental *in vivo* data presented in the paper by Hermans *et al.* [18]. This paper indicates that the lenticular volume of five subjects between 18 and 35 years of age is in the range 150–165 mm^3. A study of 27 isolated eyes between 6–82 years old in a paper by Urs *et al.* [34] provides a regression of volume versus age, giving a volume of 172.06 ± 11.31 mm^3 for the 30 year old eye. The smaller volume given for our example could be attributed to the relatively small value for unaccommodated lens thickness, $T_0 = 3.18$ mm. A study by Koretz and co-workers suggests that the 30 year old lens' thickness is in the range 3.52–3.67 mm, based on MRI and Scheimpflug imaging, respectively [35]. For this thickness range, the volume of our lens example would be 154.2–167.9 mm^3, which is in line with experimental data.

The theoretical values for surface area show the expected decreasing trend with accommodation. The surface area decrease was calculated as 3.28% over 6 D, which is comparable to the experimental MRI estimate of $4.78\% \pm 2.29\%$ over the same accommodative range (0–6 D) in the study by Hermans *et al.* [18]. This study gives values of 175.9 ± 2.8 mm^2 and 167.5 ± 2.9 mm^2 for the unaccommdated and 6 D accommodated lens, respectively. The regression formula for 27 isolated lenses provided in Urs et al. [34] gives a value of 170.5 ± 9.2 mm^2; usually, the isolated lenses assume the fully accommodated state. At 6 D, our model predicts a value of 147.6 mm^2; however, our initial lens is relatively thin, with a thickness of only 3.18 mm. Bringing the initial lens thickness to average values provided in Koretz *et al.* [35] of 3.52–3.67 mm would produce a surface area of 167.3–176.1 mm^2 at 6 D. Hence, the initial surface area of our model, and area decrease with accommodation, are comparable to the experimental findings.

For 30 isolated lenses aged 20–69, Urs et al. [36] provide a regression formula for lenticular diameter, giving a value of 9.2 ± 0.6 mm for the 30 year old lens. For the *in vivo* lens, the study of Jones *et al.* [19] gives a per-dioptre change in diameter of -0.067 ± 0.030 mm/D, corresponding to -0.402 ± 0.180 mm over 6 D. Their average unaccommodated diameter is given as 9.33 ± 0.33 mm; this represents a percentage decrease in diameter of $4.29\% \pm 1.93\%$ over 6 D. The diameter of our lens example decreases by 2.52% over the same 6 D. This decrease in diameter with accommodation, together with the initial value of 9.0 mm, is within the range of experimental data.

5. Analysis of lenticular optical power and spherical aberration

It is worth noting that Eqs. 7 were generated for accommodative amplitude of the *whole* eye. Taking the cornea and lens as two refracting surfaces in a simplified schematic eye, their relative separation implies that a total *ocular* power change of 8 D requires a *lenticular* power change of approximately 10 D. An approximate thin-lens equation—differing by only 1.4% from the exact equation—was used to verify the change in lenticular power F versus accommodation [13]:

$$F = \frac{n_s - n_{aq}}{R_a} + \frac{2P}{2P-1}(n_c - n_s)\left(\frac{1}{R_a} + \frac{1}{R_p}\right) + \frac{n_s - n_{vit}}{R_p},$$

where n_{aq} and n_{vit} are the refractive indices of the aqueous and vitreous, respectively ($n_{aq} = n_{vit} = 1.336$), and the radii R_a and R_p are given in metres; P is the exponent characterising the GRIN structure of the lens. Table 1 indicates the approximate 10 D lenticular power change between the minimally and maximally accommodated states, in accordance with the 8 D total ocular power change. Note that a 30 year old subject might not be able to accommodate by 8 D, due to the onset of presbyopia. Taking into account accommodative lag and expected

#202310 - $15.00 USD Received 3 Dec 2013; revised 19 Feb 2014; accepted 18 Mar 2014; published 28 Apr 2014

accommodative ability at 30 years of age, the model probably overestimates the change in lens power of the 30 year old lens.

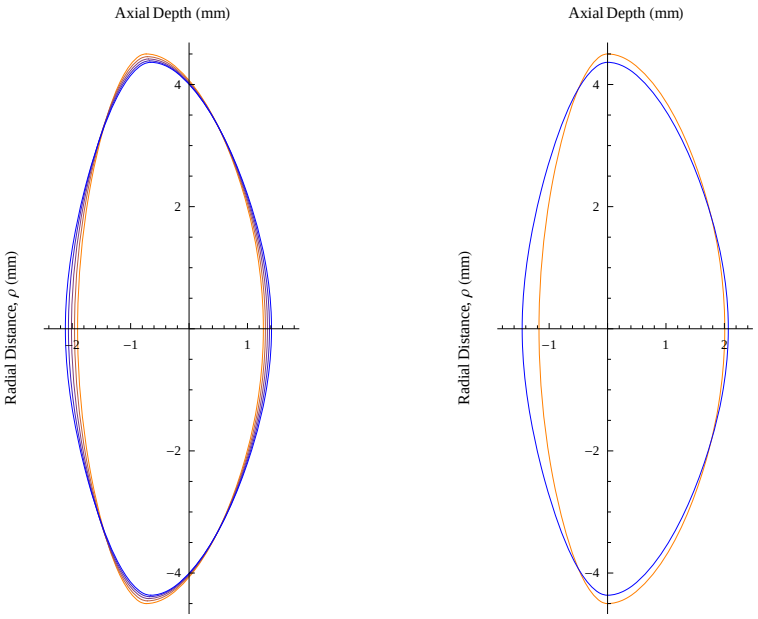

(a) Nucleus as the unmoving reference point. (b) Equator as the unmoving reference point.

Fig. 2: Lens profile for ocular accommodative amplitudes from 0D (orange) to 8D (blue).

Further validation of the method was achieved through calculation of the total lenticular spherical aberration (SA). It is clear that an accurate model of the human crystalline lens will need to account for the trend in lenticular SA as well as the change in refractive power. Total ocular SA is known to become less positive with accommodation [10, 37–49], a trend first observed by Young in 1801 [50]; see Table 3 for a summary of recent experimental data for changes in ocular SA (Zernike coefficient Z_4^0). However, the change in lenticular SA with accommodation is not widely documented in the literature—most studies report changes in total ocular aberrations only. In general, it is difficult to disentangle the SA contribution of the human lens from that of the cornea when measuring *in vivo*. In the majority of cases, no distinction is made between the posterior corneal surface and the lens, so that the optical effects of these internal optics are considered together. In this case, the lenticular SA is found as the difference between ocular and anterior corneal SA, as in the study by Li *et al.* [49]. Despite this limitation, we shall try to compare the lens model prediction with experimental data.

Before calculating the SA output of the current tool, it was first necessary to assess the contribution of conic constant to SA. According to the third-order theory applied in this paper, the SA of a surface or GRIN medium depends only on radius and conic constant. This definition is fine for surfaces which are pure conicoids of revolution, or when the pupil size is limited to the paraxial region. The solid blue curve in Fig. 4 shows the change of the SA wavefront aberration coefficient $(W_{4,0})$ calculated using the first Seidel sum (S_{I}) [13]:

$$W_{4,0} = \frac{1}{8} S_{\mathrm{I}}.$$

The total SA of our analytical lens model was calculated from the anterior and posterior

#202310 - $15.00 USD Received 3 Dec 2013; revised 19 Feb 2014; accepted 18 Mar 2014; published 28 Apr 2014

Table 3: Experimental changes in lenticular and ocular SA (Z_4^0) per dioptre. All data are scaled down to a 3 mm pupil diameter from their measured pupil diameters (given in mm).

Study	Meas. pupil	ΔSA (Z_4^0) (μm/D)	Age ± SD (Range)	# Eyes	Accomm. range (D)
[a] Li *et al.* [49] SRR[b]	3	−0.0043	21 ± 2.5 (19–25)	82	2.5
	5	−0.0068			
Ninomiya *et al.* [43] HS[c]	4	−0.0032	29 ± 4.4	33	3
	6	−0.0023			
López-Gil *et al.* [51] HS	4	−0.0035	21 ± 2.3 (19–29)	12	5
	4	−0.0060	36 ± 1.6 (30–39)	13	5
Cheng *et al.* [45] HS	5	−0.0056	25 ± 4 (21–40)	76	6
He *et al.* [42] SRR	6.25	−0.0035	29 ± 4.5 (24–38)	8	6

[a]Lenticular SA; [b]SRR, Spatially Resolved Refractometer; [c]HS, Hartmann–Shack.

surfaces, and the GRIN structure whose profile was defined by $P = 2.94$ for the 30 year old eye, in accordance with the work of Navarro *et al.* [15]; this P-value is also within the range reported by Kasthurirangan *et al.* [52]. The corresponding iso-indicial contours are shown in Fig. 1. The lens was analysed with a collimated entrance beam in a medium with refractive index of 1.336, with $n_c = 1.416$ and $n_s = 1.376$, and a 2.66 mm iris diameter. Note that a 2.66 mm iris corresponds approximately to a 3 mm entrance pupil diameter due to typical corneal magnification of approximately 1.13 [7]. SA was calculated using the figuring conic constants K_a and K_p provided in Table 2. The SA ($W_{4,0}$) of the lens at 0 D was -0.0880 μm, and for the accommodation range of 0–2 D, a linear fit of the plot gave a slope of $\Delta W_{4,0} = -0.0677$ μm/D. This calculation is only valid for small pupil diameters. Comparison with the experimental data for pupil diameters of 3 mm and greater, in Table 3, requires an extension of the third-order theory calculation to intermediate pupil diameters.

To extend the validity of the third-order theory, we have to account for the figuring conicoid functions including the B-coefficient contribution to SA. Thus it is necessary to reconsider our description of the surface shape at intermediate pupil heights. When using only pure conicoids to represent the lens' surfaces, the conic constant is responsible for the overall shape of the lens at large heights. It has been shown that the lens shape is more complex than this simple conicoid [53–55]. To provide more realistic lens shapes, we use a figuring conicoid featuring a higher-order aspheric term and B-coefficient; see Eq. 1.

The method employed in the work of Dubbelman *et al.* (2005) [24] was to fit a pure conicoid function to the experimental images of the lens' surface over a 6 mm diameter; this gave an approximation to the true, highly-aspheric shape of the lens' surface, with associated approximate conic constant for that surface. However, if a figuring conicoid was used, the B-coefficient would assume a certain value, and would alter the value of the approximate conic constant determined initially. The conic constants obtained using the B-coefficient are figuring conics K_a and K_p, which are suitable for use in third-order aberration analysis with small pupils.

However, to approximate the central and intermediate region of the lens, we need to modify the conic constants so that the pure conicoid of revolution more closely follows the figuring conicoid's aspheric surface. The modified values for the conic constants (K_a^* and K_p^*) can be derived by choosing ρ_1 and solving equation Eq. 1 for a corresponding sag, z_1, that defines the

#202310 - $15.00 USD Received 3 Dec 2013; revised 19 Feb 2014; accepted 18 Mar 2014; published 28 Apr 2014

point (z_1, ρ_1) at which our new, pure conicoid will intersect the figuring conicoid:

$$\rho_1^2 = 2Rz_1 - (1+K)z_1^2 + Bz_1^3.$$

The approximate conic constant can be found by solving for K^* in the equation:

$$\rho_1^2 = 2Rz_1 - (1+K^*)z_1^2, \quad \text{thus:} \quad K^* = K - Bz_1.$$

Table 2 contains the figuring and approximate conic constants predicted by the current tool. Note that the approximate conics were obtained by fitting (a pure conicoid) to the lens' surface at a height $\rho_1 = 2.5$ mm, which corresponds to the point M_a in Fig. 3. This height was chosen so that the internal iso-indicial contours of the GRIN structure which have not yet plateaued to the central refractive index are still suitably approximated by the pure conicoid for ray-tracing at 3 mm pupil diameter. For example, we can see in Fig. 3 (a) that the ray at entrance pupil height of 1.5 mm intersects the internal contour at point M_{in} at a height that is scaled down from the initial 2.5 mm height of the point M_a on the external surface. Fitting at larger heights would deteriorate the quality of the fit; thus, analysis at very large heights requires numerical ray-tracing.

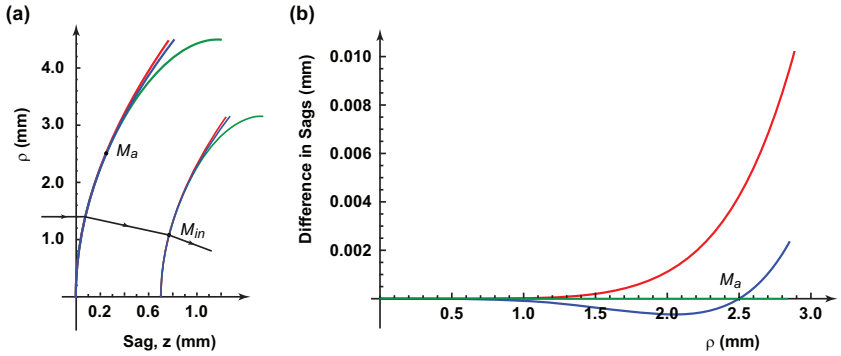

Fig. 3: Fitting the figuring conicoid (green) with a pure conicoid (blue) of conic constant K_a^* at intersection point M_a, $\rho = 2.5$ mm (a). The red curve is a pure conicoid with conic constant K_a; (b): the difference in sag between green, red and blue curves for different lens heights.

Now, SA can be calculated for a 3 mm pupil diameter using these approximate conic constants K_a^* and K_p^*, which are provided in Table 2. The change of SA versus accommodation is given by the solid black curve in Fig. 4. From this figure, we can see that the lenticular SA predicted by the current tool—when using the approximate conics—decreases at a slower rate than with the figuring conics (blue curve). This is because the approximate conics are less negative than the figuring conics; see Table 2. Experimental data for the accommodative change in ocular and lenticular SA is provided in this Fig. 4; error bars are given where data were available. Where relevant, experimental data for SA (Zernike coefficient Z_4^0) are scaled to a 3 mm pupil. Assuming that the corneal contribution to ocular SA is constant with accommodation, the rate of change of ocular SA versus accommodation is directly related to the rate of lenticular SA change. Lenticular SA (given as internal optics) was available in the study by Li *et al.* only. The rate of change in the Zernike coefficient Z_4^0 is provided in Table 3, which is converted to $W_{4,0}$ in Fig. 4 for comparison with the third-order model prediction:

$$W_{4,0} = 6\sqrt{5}Z_4^0.$$

With the approximate conics, the predicted lenticular SA agrees with the well-known trend of decreasing SA with accommodation (becoming more negative). Validation of the tool was

#202310 - $15.00 USD Received 3 Dec 2013; revised 19 Feb 2014; accepted 18 Mar 2014; published 28 Apr 2014

extended by analysing the decrease of SA per dioptre over a range of accommodative amplitudes. That is, the decreases in SA over the ranges 0–2 D, 0–4 D, 0–6 D and 0–8 D were each fitted with a line. The slopes of these linear fits are provided in Table 2. Given the size of the error bars and noticeable spread in experimental data [10], the decrease in Zernike Z_4^0 predicted by the current tool is in agreement with the data listed in Table 3. The predicted rate of change in SA is in line with experimental data for the available accommodative range of 0–6 D. For this range, the output of the model shows a non-linear trend. Fitting with a second-order polynomial gives: $W_{4,0}(A) = 0.0262 - 0.0128A - 0.0145A^2$, where A is accommodation in dioptres.

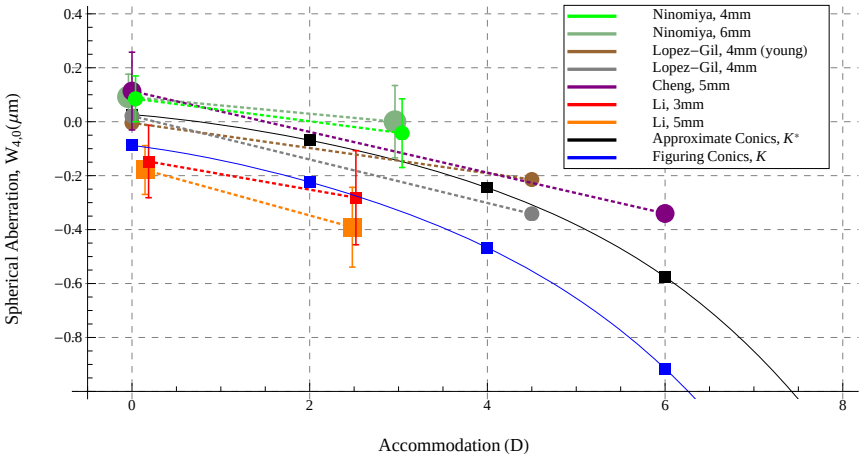

Fig. 4: Change in ocular (disks) and lenticular (squares) SA; marker size indicates measured pupil diameter. All data are scaled to 3 mm pupil, and are compiled from Tables 2 & 3.

The unaccommodated lens with approximate conics shows a value of SA $(W_{4,0}) = 0.0262$ μm, which corresponds to the Zernike coefficient of primary SA: $Z_4^0 = W_{4,0}/(6\sqrt{5}) = 0.0020$ μm. This value is slightly positive, while the value obtained using the figuring conics is negative $(W_{4,0} = -0.0880$ μm); this negative value is valid for much smaller pupil diameters. Typically, the human lens shows a negative value at 0 D. Studies have found that, in general, positive corneal SA is partly cancelled by negative SA of the lens or internal optics [56–65]; we stress here the generality of those results. However, a paper by Millodot and Sivak shows that the lenticular SA generally adds to that of the cornea [66]. Papers by Artal *et al.* and Glasser and Campbell show compensation in young eyes, with augmentation in older eyes [67, 68]. Furthermore, more recent papers by He *et al.* [69], and Salmon and Thibos [70] show both compensatory and additive roles of the internal optics in ocular SA production. A paper by He *et al.* shows that the lens reduces the total RMS wavefront aberration of the cornea, but individual Zernike corneal aberrations were not always compensated by the lens [71]. Kelly and co-workers also found that corneal SA was not always reduced by the lens [64].

We can see that there is large inter-subject variability in the experimental values for the SA of internal optics at 0 D; thus, we should not expect that lenticular SA is always negative. For the particular choice of initial lens geometry for this model [25], the value of lenticular SA at 0 D is slightly positive when analysing the lens at a 3 mm pupil. More important is the trend in SA with accommodation, which is in agreement with experimental data. The approximating conics are more valid for this intermediate pupil diameter.

These approximate conics can be compared to those reported in the work of Dubbelman *et al.* (2005) [24]. Therein provided is a linear regression for the change per dioptre in conic of

#202310 - $15.00 USD Received 3 Dec 2013; revised 19 Feb 2014; accepted 18 Mar 2014; published 28 Apr 2014

the lens' anterior surface, as a function of the anterior conic at 0 D, K_{0a}:

$$\Delta K_a = (-0.63 - 0.07 \times K_{0a})A,$$

where A is accommodation in dioptres. For this, we use $K_{0a}^* = -0.83$, corresponding to an experimental $\Delta K_a^* = -4.58$ over 8 D; this can be compared with the change $\Delta K_a^* = -5.79$ predicted by the current tool, and given in Table 2.

6. Discussion and conclusion

The modelled change in SA with accommodation is an important finding, since it represents the first clear understanding of how lenticular SA can decrease with accommodation according to Helmholtz's theory. It is widely known that increasing surface curvatures cause more positive SA, and so the accommodative decrease in lenticular radii should produce more positive SA. With this tool, we can analytically predict that the conic constants become more negative, and this in turn gives more negative SA of the lens. Our method employs the simple physical lens constraints of constant volume and fixed equator to analytically solve for the conic constants. With these conic constants, we calculate the accommodative changes in SA by ray-tracing through the lens' GRIN medium. Since the GRIN medium follows the external surface geometry, this model takes into account both surface asphericity and GRIN structure when calculating lenticular SA.

The change in lenticular SA *in vivo* with accommodation is not widely documented in the literature, since it is difficult to disentangle the SA contribution of the human lens from that of the cornea; most studies report changes in total ocular aberrations only. Usually, the optical effect of the posterior cornea and lens are considered together. In this case, the lenticular SA is found as the difference between ocular and anterior corneal SA. In spite of this obvious limitation, we have compared the lens model prediction with experimental data, and found that the model prediction is in agreement with the data.

With this method, it is possible to predict analytically the accommodative changes in various lenticular parameters such as surface area, equatorial diameter, refractive power and SA. We invite others to use this tool for future refinement as new data become available.

An important aspect of this new method is the constancy of lenticular volume with accommodation. With the derived formulae for figuring conic constants, it is possible to preserve the volume of the lens when modelling in ray-tracing software, where the specification of volume is currently not directly available. This will therefore allow modelling of a physically realistic lens in ray-tracing software, and give new insight into the accommodative process. If the conic constants of the lens are given as a function of accommodation, one could revisit the dependency on experimental data for accommodative changes in lenticular radii and thickness, and instead use these geometrical parameters to keep the lens' volume constant. Moreover, if it is found that the lenticular volume is not constant with accommodation, one could relax the constant volume condition.

The future aim of ocular modelling is the development of a model which characterises the geometrical, optical and biomechanical properties of the ageing lens lens under accommodation [72]. We hope that an understanding of how the geometrical and optical properties of the lens change with accommodation will help to consolidate, in future, more information regarding the accommodation process.

Acknowledgements

The authors wish to acknowledge the funding of The Irish Research Council Embark Initiative, application RS/2012/351. This research was also supported by Fight for Sight under grant 1319/1320.

#202310 - $15.00 USD Received 3 Dec 2013; revised 19 Feb 2014; accepted 18 Mar 2014; published 28 Apr 2014